NiCoP nanoparticle-decorated carbon nanosheet arrays assembled on nickel nanowires for volumetric-energy-dense supercapacitors

Min Hong[*, a†], Bingcheng Luo [c†], Chao Zhou [b], Shusheng Xu [b], Liying Zhang [b], Zili Zhang [d], Zhi Yang [b], Nantao Hu[*, b], Yafei Zhang [b], Zheng Liang[*, a]

a Frontiers Science Center for Transformative Molecules, School of Chemistry and Chemical Engineering, Shanghai Jiao Tong University, Shanghai 200240, China

b Key Laboratory of Thin Film and Microfabrication Technology (Ministry of Education), School of Electronics, Information and Electrical Engineering, Shanghai Jiao Tong University, Dong Chuan Road No.800, Shanghai, 200240, P. R. China

c College of Science, China Agricultural University, Beijing 100083, China

d School of Science, China University of Geosciences, Beijing 100083, China
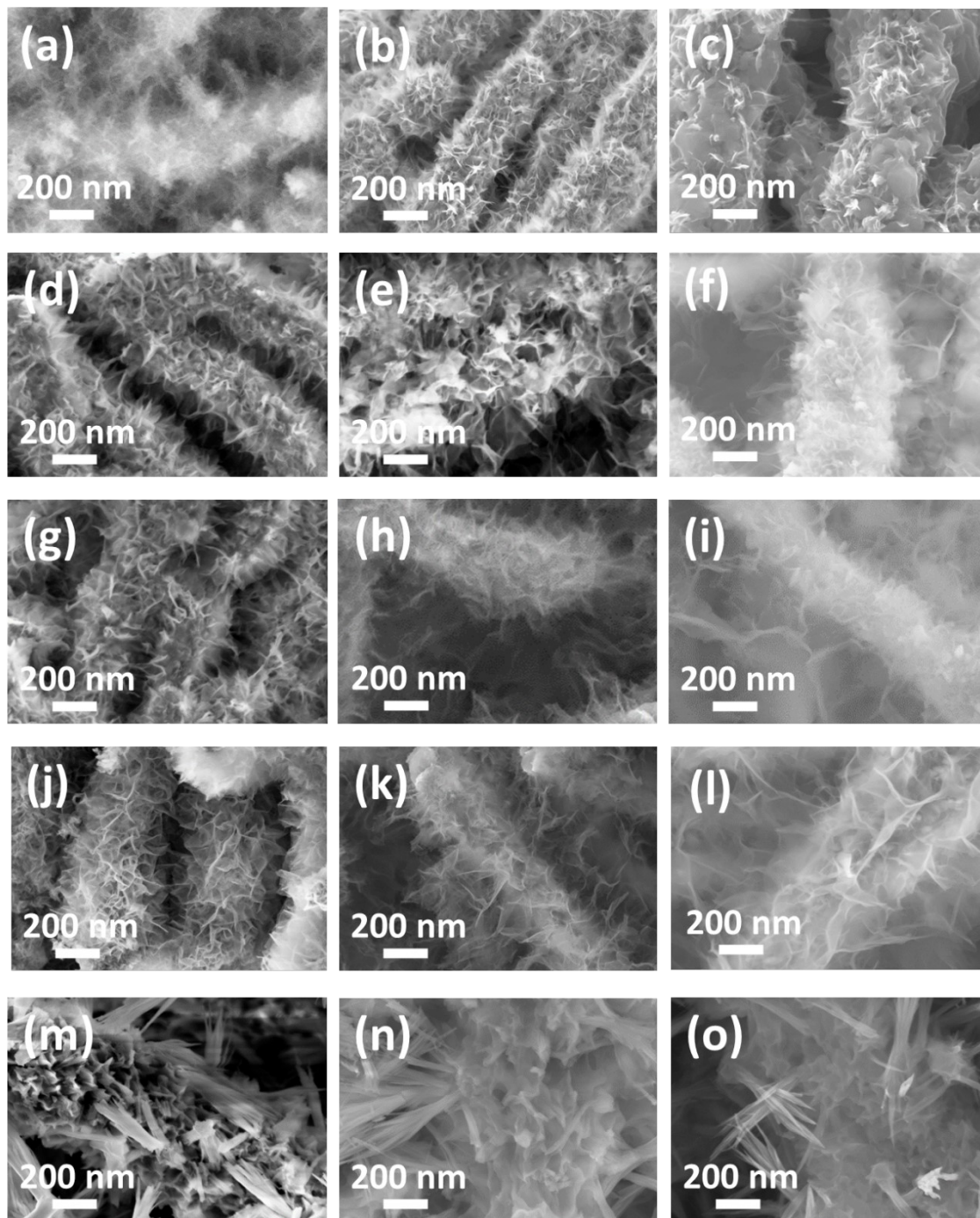
†These authors contributed equally.

Figure S1. SEM images of Ni@NiCo-OH electrode at (a) hydrothermal, (b) thermal annealed, and (c) phosphide state. SEM images of Ni@PDA-NiCo electrode with DA precursor content of (d) 0.05 M, (g) 0.1 M, (j) 0.2 M, (m) 0.4 M, and the corresponding (e, h, k, n) carbonized and (f, i, l, o) phosphide state.
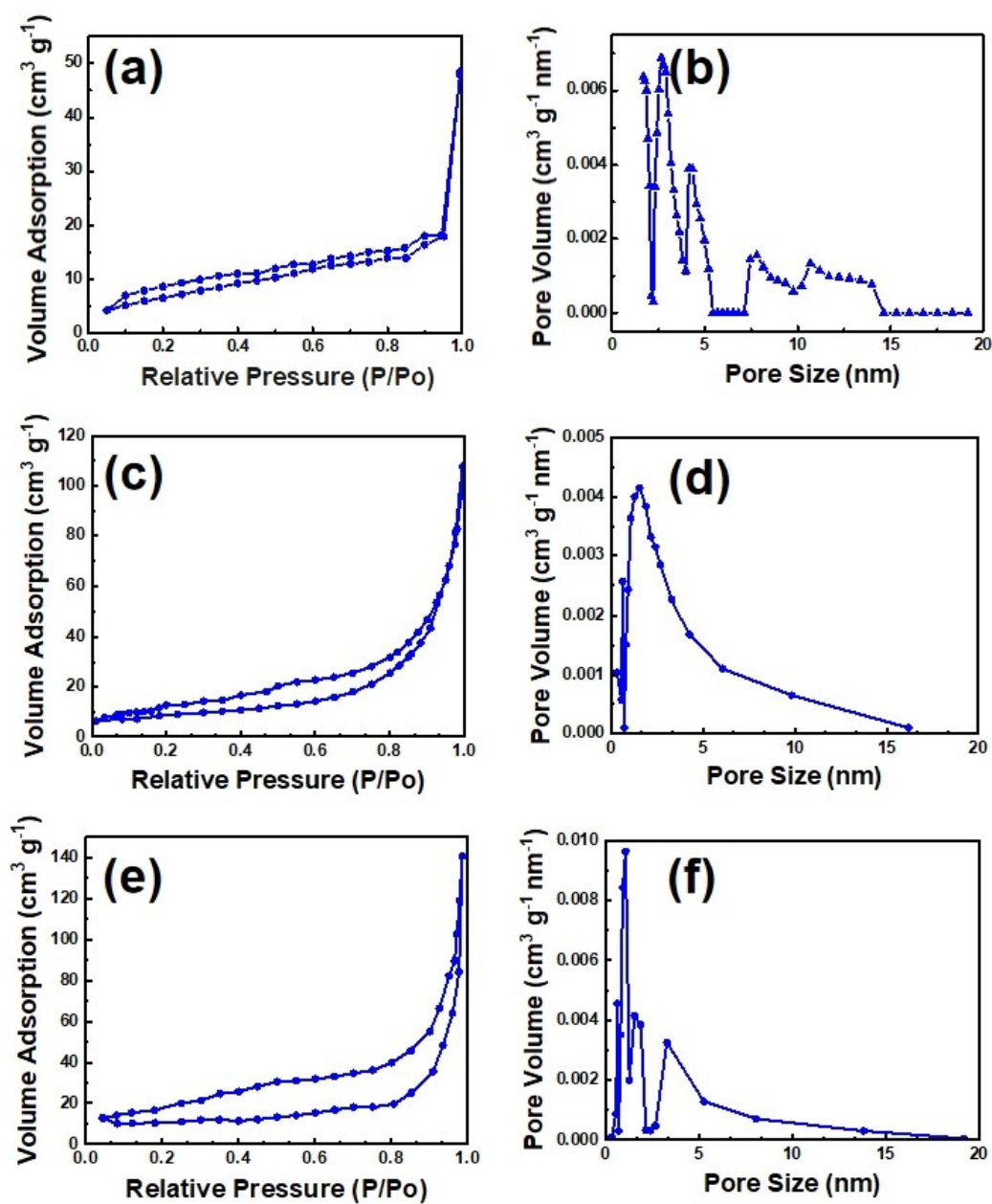
Figure S2. (a, c, e) Nitrogen adsorption/desorption isotherm and (b, d, f) pore size distribution curve of pristine Ni film, Ni@PDA-NiCo, and Ni@C-NiCoO electrodes, respectively.
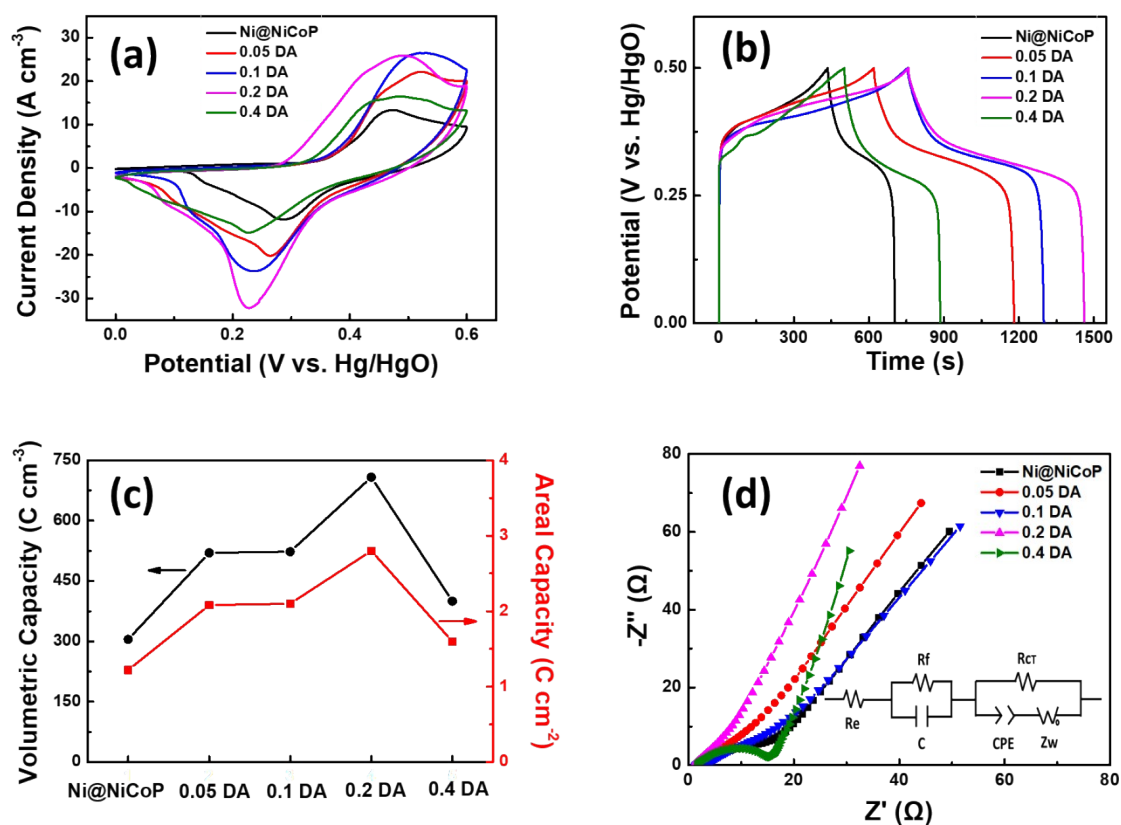
Figure S3. Electrochemical properties. (a) CV curves (10 mV s^{-1}) of Ni@C-NiCoP electrodes with DA precursor content from 0 to 0.4 M. (b) Corresponding GCD curves at 1 A cm^{-3}. (c) Volumetric and areal specific capacity calculated from GCD curves at 1 A cm^{-3}. (d) EIS curves of four electrodes. Inset is the Equivalent circuit for EIS fitting.
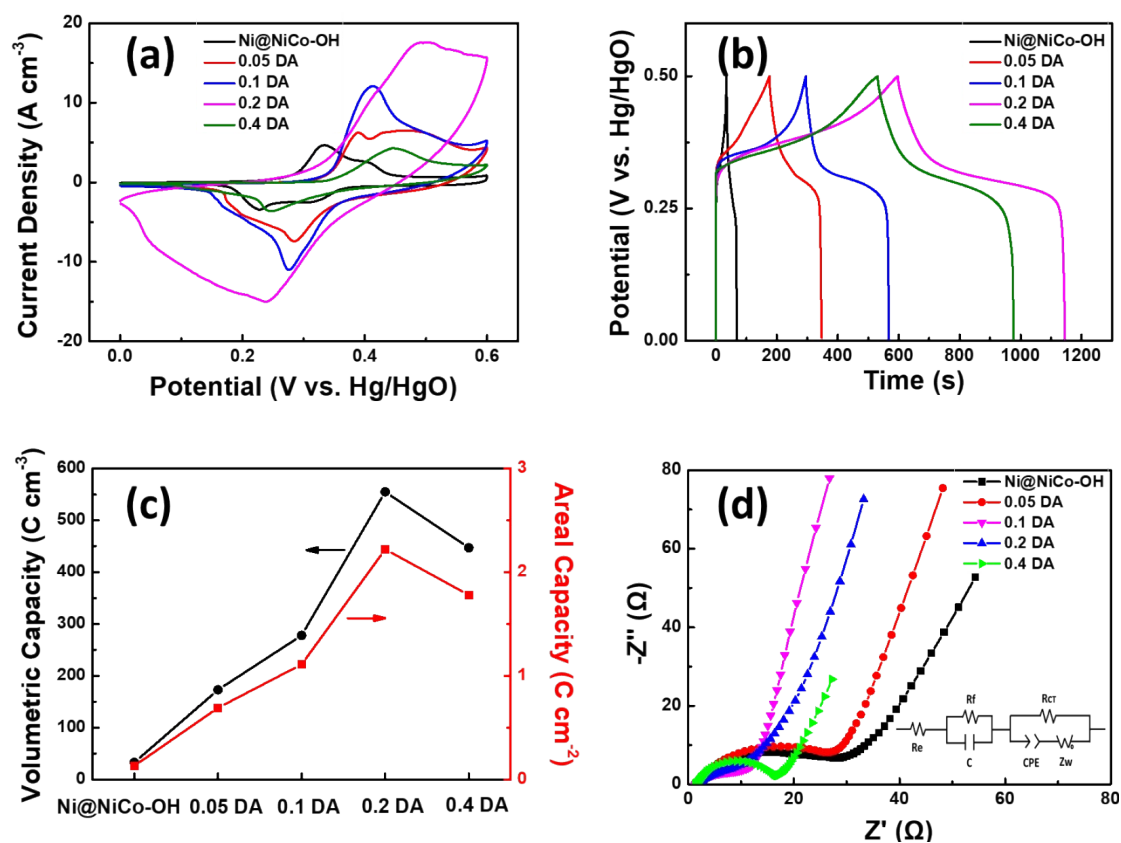
Figure S4. Electrochemical properties. (a) CV curves (10 mV s⁻¹) of hydrothermal processed Ni@NiCo-OH electrodes with DA precursor content from 0 to 0.4 M. (b) Corresponding GCD curves at 1 A cm⁻³. (c) Volumetric and areal specific capacity calculated from GCD curves at 1 A cm⁻³. (d) EIS curves of four electrodes. Inset is the fitted Equivalent circuit.
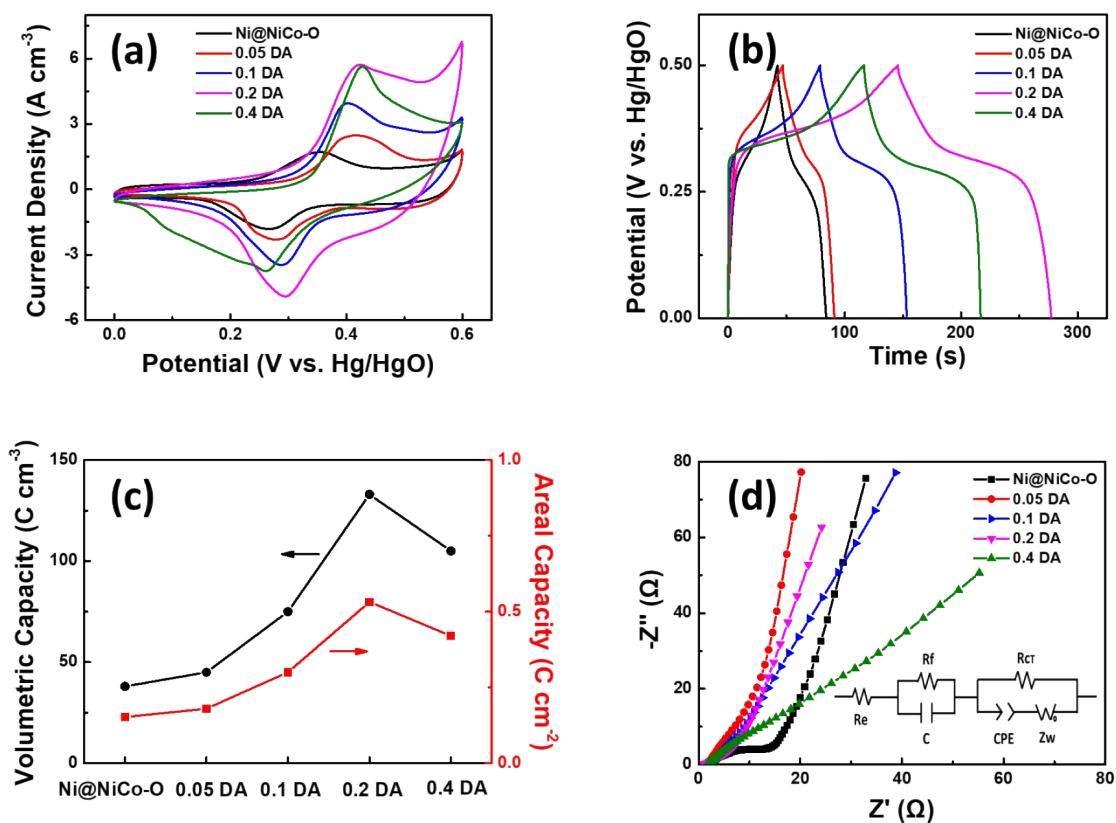
Figure S5. Electrochemical properties. (a) CV curves (10 mV s^{-1}) of carbonized Ni@C-NiCoO electrodes with DA precursor content from 0 to 0.4 M. (b) Corresponding GCD curves at 1 A cm^{-3}. (c) Volumetric and areal specific capacity calculated from GCD curves at 1 A cm^{-3}. (d) EIS curves of four electrodes. Inset is the Equivalent circuit for EIS fitting.
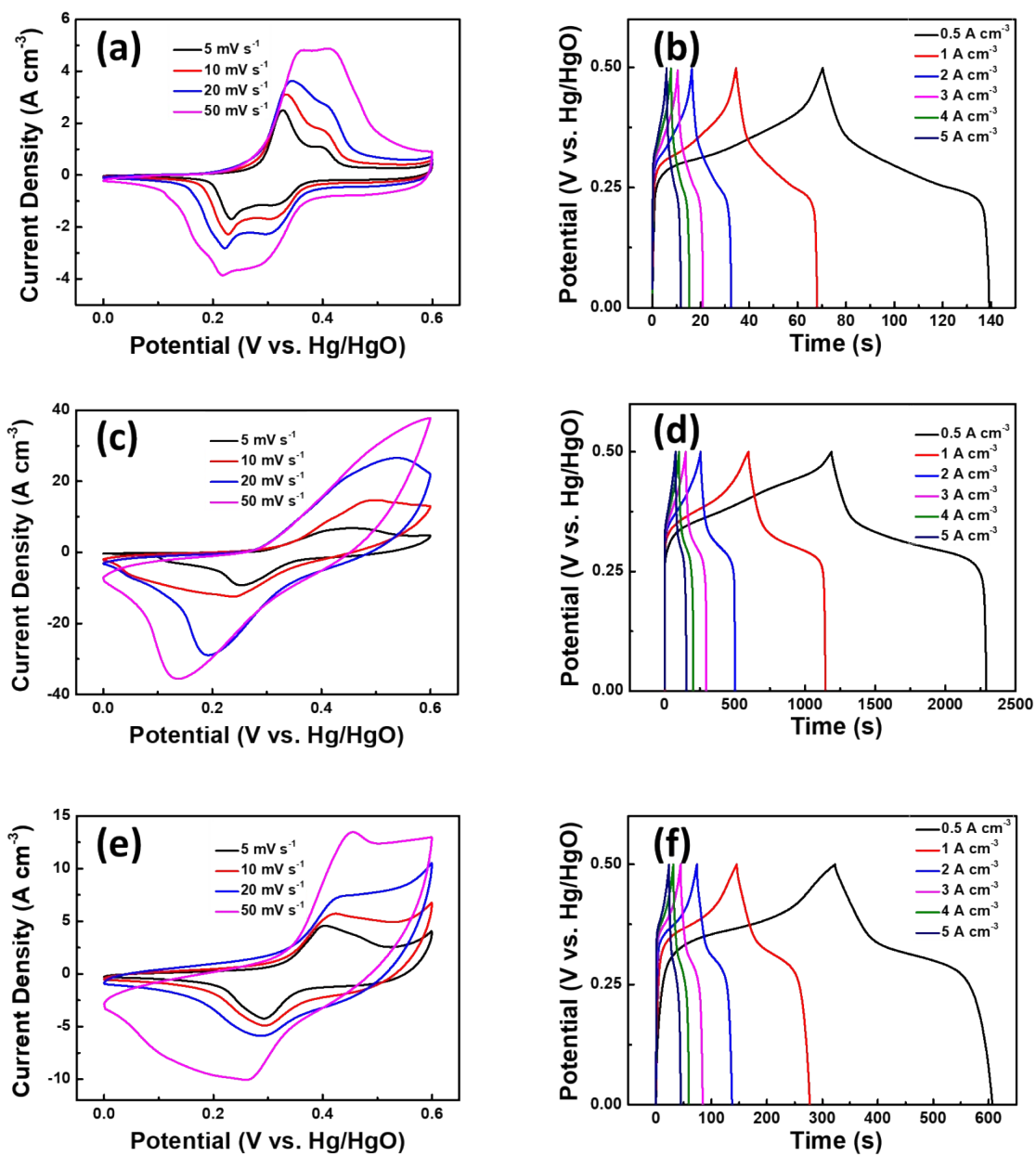
Figure S6. CV (5 to 50 mV s^{-1}) and GCD (0.5 to 5 A cm^{-3}) curves of (a, b) Ni@NiCo-OH, (c, d) Ni@PDA-NiCo, (e, f) Ni@C-NiCoO electrodes, respectively.

Table S1. Electrochemical performance comparison between Ni@C-NiCoP and other phosphide-based electrodes.

| Material	Electrolyte	Volumetric Capacity (C/cm³)	Rate Capacity (C/cm³)	Reference
NiCoP/MXene	3 M KOH	40 (0.6 A/cm³)	35 (1 A/cm³)	[1]
NiCoP@NiCoP	KOH/PVA	667 (1 A/cm³)	534 (40 A/cm³)	[2]
aPC@CoP-CC8	2 M KOH	26 (0.15 A/cm³)	18 (0.75 A/cm³)	[3]
NiCoP/NF	6 M KOH	245 (0.2 A/cm³)	/	[4]
FeP/PEDOT	1 M Na$_2$SO$_4$	225 (0.1 A/cm³)	/	[5]
NiCoP rod/NF	1 M KOH	50 (0.05 A/cm³)	46 (0.5 A/cm³)	[6]
pNiCoP/NF	6 M KOH	129 (0.1 A/cm³)	86 (1 A/cm³)	[7]
NiCoP@NiCoH/C	3 M KOH	235 (0.5 A/cm³)	150 (4 A/cm³)	[8]
Ni@C-NiCoP	6 M KOH	708 (1 A/cm³)	481 (5 A/cm³)	**This work**
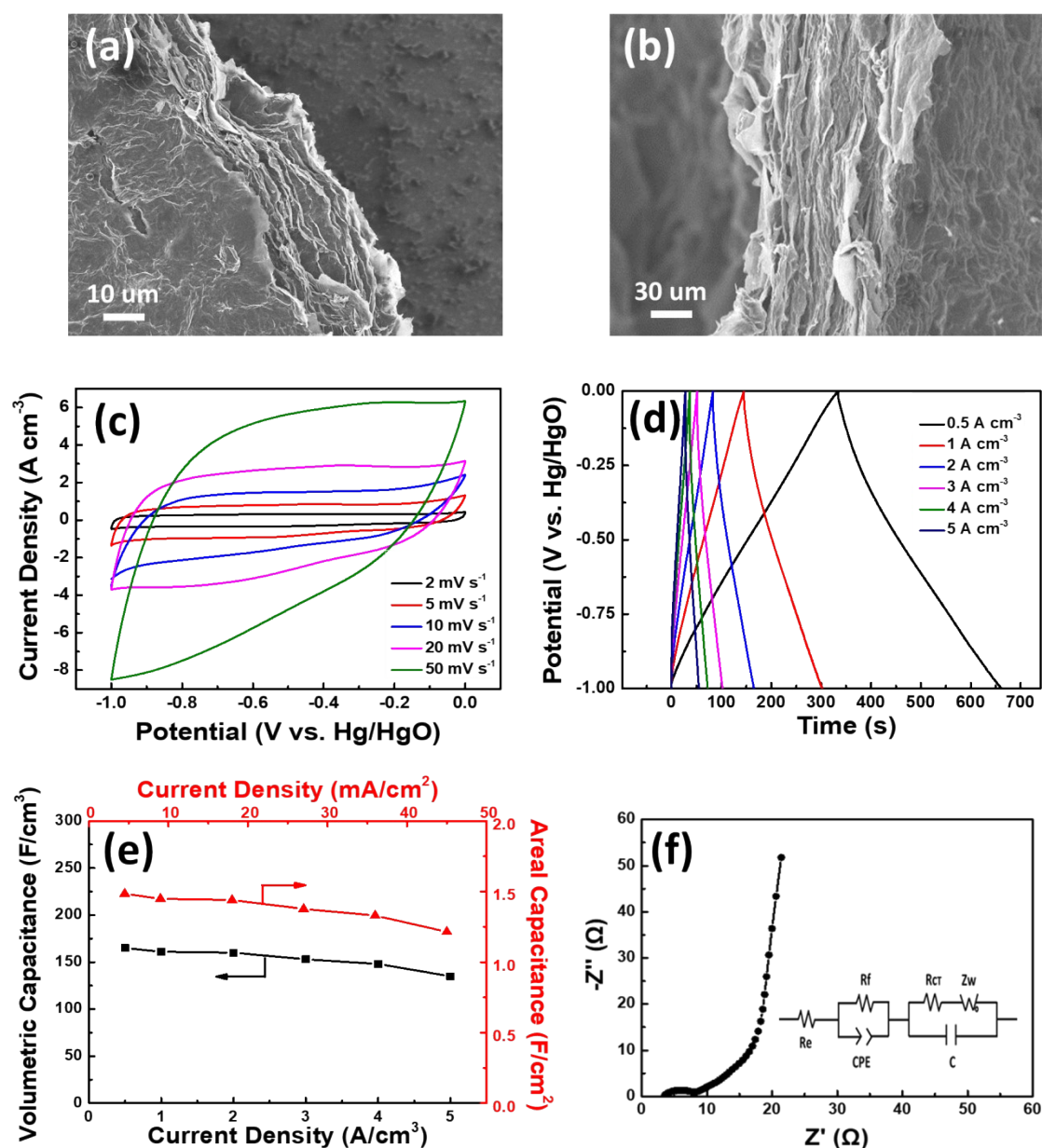
Figure S7. (a) Surface morphology of G-CNT film. (b) Cross-sectional morphology of G-CNT film. (c) CV curves of G-CNT film at scan rates ranging from 2 to 50 mV s^{-1}. (d) GCD curves of G-CNT film at various current densities from 0.5 to 5 A cm^{-3}. (e) Plots of calculated volumetric and areal specific capacitance. (f) EIS curve of G-CNT film. Insert is the equivalent circuit for EIS fitting.

Reference:

[1] L. H. Yu, W. P. Li, C. H. Wei, Q. F. Yang, Y. L. Shao, and J. Y. Sun, *Nano-Micro Lett.* 12 (2020) 143.

[2] Q. L. Liu, *Small* 17 (2021) 2101617.

[3] T. Kim, A. P. Tiwari, K. Chhetri, G. P. Ojha, H. Kim, S. H. Chae, B. Dahal, B. M. Lee, T. Mukhiya, and H. Y. Kim, *Nanoscale Adv.* 2 (2020) 4918.

[4] C. X. Zhou, T. T. Gao, Y. J. Wang, Q. L. Liu, and D. Xiao, *Appl. Surf. Sci.* 475 (2019) 729-739.

[5] J. L. Luo, Z. Zheng, A. Kumamoto, W. I. Unah, S. K. Yan, Y. H. Ikuhara, X. Xiang, X. T. Zu, and W. L. Zhou, *Chem. Commun.* 54 (2017) 794.

[6] Z. N. Wang, H. Wang, S. Ji, X. Y. Wang, P. X. Zhou, S. H. Huo, V. Linkov, and R. F. Wang, *Mater. Des.* 193 (2020) 108807.

[7] Z. H. Huang, X. Q. Li, X. X. Xiang, T. T. Gao, Y. J. Zhang, and D. Xiao, *J. Mater. Chem. A* 7 (2019) 24374.

[8] C. P. Duan, L. L. Wang, J. P. Liu, Y. N. Qu, J. Gao, Y. Y. Yang, B. Wang, J. H. Li, L. L. Zheng, M. Z. Li, and Z. Yin, *ChemElectroChem.* 8 (2021) 2272-2281.